Prime Geometry XIII: Solution Theory, Stability Classes, and the Geometry of PGME Flows

Allen Proxmire

December 2025

Abstract

Prime Geometry XII introduced the Master Equation of Prime Geometry, a coupled second-order evolution law unifying curvature, angle drift, angle deviation, and the global curvature–energy potential into a single dynamical structure governing the prime gap sequence. While PG12 formulated this equation and demonstrated its ability to reproduce the local, mesoscopic, and global geometric behavior of the primes, the deeper question remains: what types of sequences actually arise as solutions of this system?

Prime Geometry XIII develops the first solution theory for the Prime Geometry Master Equation (PGME). We analyze the equation as a discrete geometric flow, identify stability regimes, classify admissible solution types, reconstruct the empirical attractor occupied by the prime gaps, and characterize how coherence phases, curvature suppression, and angle stability emerge naturally as dynamical consequences of the PGME. The goal is not prediction, but understanding the structure of the solution space itself: why the primes follow a uniquely stable trajectory within it, and how deviations are corrected or amplified depending on their geometric character.

PG13 establishes Prime Geometry as a dynamical system with well-defined stability classes, attractor geometry, and constrained flow behavior, forming the theoretical foundation for the analytic and spectral developments of PG14 and beyond.

1 Introduction

Prime Geometry XIII marks the transition from formulating the dynamical laws of prime evolution (PG9–PG12) to analyzing the *solution space* of those laws. The Prime Geometry Master Equation (PGME), introduced in PG12, unifies the first- and second-order geometric derivatives of the prime gap sequence—curvature χ_n, angle drift $\Delta\alpha_n$, and angle deviation $\alpha_n - \pi/4$—with a global curvature–energy potential $\Phi(n)$ derived from the low-action structure of the primes. The resulting evolution equation captures the essential features documented throughout PG1–PG11: suppressed curvature, extended coherence phases, smooth angle evolution, controlled transitions, and a global dynamical balance between expansion and contraction.

The present paper asks the natural next question:

> *What behaviors does the PGME actually allow? Which are stable, which are unstable, and why do the true primes occupy a specific, highly constrained region of the solution space?*

To address this, PG13 develops the first detailed analysis of the PGME as a discrete geometric dynamical system. We study local perturbations, mesoscopic coherence regimes, global stability

inequalities, renormalized scaling behavior, and the structure of the attractor that emerges when PGME trajectories are viewed in the (g_n, g_{n+1}, χ_n) state space. Through both analytic reasoning and numerical reconstruction, we show that the PGME possesses a narrow class of *prime-like* solutions characterized by low curvature, balanced signed curvature, third-order smoothness, and extremely stable angle behavior. Most theoretical trajectories do not share these properties, revealing that the primes constitute a special, highly structured flow within a vastly larger geometric possibility space.

Prime Geometry XIII therefore serves as the solution-theoretic companion to the PGME. It establishes the stability classes, attractor geometry, and flow dynamics needed to understand how the prime gaps evolve, why continuity and coherence persist over long ranges, and how the global constraints identified in PG7–PG12 govern the entire system. This sets the foundation for PG14, which will develop the analytic structure of the PGME potential, and PG15, which will explore the extension of the PGME framework to the geometry of zeta-zero gaps.

2 The PGME as a Geometric Dynamical System

Prime Geometry XII introduced the Master Equation (PGME) as the unified second-order dynamical law governing the evolution of the prime gap sequence. In this section we reinterpret the PGME as a discrete geometric flow acting on a state vector that encodes the local and global geometric structure of the primes. This framing will serve as the basis for the stability, classification, and attractor analyses developed in later sections.

2.1 State Variables and the Evolution Map

Let $g_n = p_{n+1} - p_n$ denote the prime gaps, and let χ_n, $\Delta\alpha_n$, and $\Phi'(n)$ be the curvature, angle drift, and potential gradient, respectively, as defined in PG5–PG12. We package these into the geometric state vector

$$X_n = \big(g_n,\ g_{n+1},\ \chi_n,\ \Delta\alpha_n,\ \Phi'(n)\big).$$

The PGME expresses g_{n+2} as a function of the components of X_n:

$$g_{n+2} = g_n + A(g_n, g_{n+1})\,\chi_n + B(p_n)\,\Delta\alpha_n + C\,\Phi'(n) + \varepsilon_n, \tag{1}$$

where $A(g_n, g_{n+1}) \approx g_n + g_{n+1}$, $B(p_n) \approx 2p_n$, and C is a small but essential global regularization coefficient. The term ε_n is a structured residual capturing geometric effects beyond the current model.

Equation (1) defines a discrete evolution map

$$X_{n+1} = F(X_n),$$

where F incorporates the recurrence for curvature, the first-order angle law, the update of the potential gradient, and the construction of g_{n+2} from X_n.

2.2 Local Structure: Curvature and First-Order Variation

The PGME combines two fundamental derivative relations established in PG5–PG6:

- **Second-order variation:**

  $$g_{n+2} - g_n = (g_n + g_{n+1})\,\chi_n,$$

  identifying curvature χ_n as a normalized second derivative.

- **First-order variation:**
$$\Delta\alpha_n \approx \frac{g_{n+1} - g_n}{2p_n},$$
expressing angle drift as a scaled first difference of the gap sequence.

The PGME unifies these by coupling the first- and second-order terms with a global potential through $C\,\Phi'(n)$, which stabilizes long-range drift and enforces the low-action structure revealed in PG2–PG4 and PG8.

2.3 Global Structure: The Curvature–Energy Potential

The potential $\Phi(n)$ introduced in PG8 encodes cumulative curvature energy:

$$\Phi(n) = \text{Smooth}\left(\sum_{k\le n} \chi_k^2\right),$$

with $\Phi'(n)$ reflecting local imbalance in curvature flow. The potential plays the role of a geometric regulator, preventing persistent drift in curvature or angle drift and constraining the system to remain near its global equilibrium geometry.

This creates a hybrid dynamical system:

(local second-order effects) + (local first-order effects) + (global stabilizing forces).

2.4 Equilibrium Geometry and Linearization

For large n, consecutive primes satisfy $p_{n+1} \sim p_n$, implying that the Prime Triangle angle α_n remains close to $\pi/4$. This motivates a linearization of the PGME around the equilibrium state

$$X^* = \big(g,\ g,\ 0,\ 0,\ 0\big),$$

which corresponds to

$$\chi_n = 0, \qquad \Delta\alpha_n = 0, \qquad \Phi'(n) \approx 0.$$

Linearization reveals the fundamental stability mechanism:

- curvature near zero forces $g_{n+2} \approx g_n$,
- small angle drift suppresses first-order variation,
- the potential gradient prevents accumulation of bias in either direction.

These effects combine to produce a restoring force that drives the state back toward the equilibrium manifold whenever perturbations arise.

2.5 The PGME as a Constrained Geometric Flow

Viewed together,

$$X_{n+1} = F(X_n)$$

defines a *constrained geometric flow* in a five-dimensional space of local and global descriptors. Not all sequences are admissible: the PGME enforces symmetry, balance, and smoothness conditions that eliminate most hypothetical trajectories.

The primes occupy a particular stable trajectory of this system. Understanding why this trajectory is preferred, and how nearby trajectories behave, is the central focus of the stability and attractor theory developed in Sections 3–5.

3 Local Stability Analysis

The Prime Geometry Master Equation (PGME) describes the evolution of the prime gaps through a coupled system of first- and second-order geometric derivatives. To understand which behaviors are admissible, we begin with a local stability analysis: how small perturbations in gaps, curvature, or angle drift influence the next steps of the system. The results of this section establish the dynamical foundation for coherence phases, third-order smoothness, and the attractor geometry developed in later sections.

3.1 Perturbations of the Gap Sequence

Let

$$g_n \longrightarrow g_n + \delta_n,$$

with δ_n small relative to $g_n \sim \log p_n$. This perturbation induces corresponding changes in curvature and angle drift:

$$\chi_n = \frac{g_{n+2} - g_n}{g_n + g_{n+1}} \quad \Rightarrow \quad \delta\chi_n = \frac{\delta_{n+2} - \delta_n}{g_n + g_{n+1}} \; - \; \chi_n \frac{\delta_n + \delta_{n+1}}{g_n + g_{n+1}} \; + O(\delta^2).$$

Thus two effects govern the sensitivity of curvature:

- **Second-order sensitivity:** differences $(\delta_{n+2} - \delta_n)$ have the strongest impact,
- **Scale damping:** the denominator $g_n + g_{n+1} \sim 2 \log p_n$ suppresses variations.

The primes benefit from this damping: random perturbations decay faster than they propagate, producing the local smoothness documented throughout PG1–PG6.

3.2 Stability of the Curvature Recurrence

Substituting perturbed curvature into the recurrence

$$g_{n+2} = g_n + (g_n + g_{n+1})\chi_n + (\text{first-order + potential terms})$$

yields

$$g_{n+2} + \delta_{n+2} = g_n + \delta_n + (g_n + g_{n+1})(\chi_n + \delta\chi_n) + \cdots .$$

Expanding and retaining first-order terms,

$$\delta_{n+2} = \delta_n + (g_n + g_{n+1})\, \delta\chi_n + O(\delta^2).$$

Using the expression for $\delta\chi_n$ above, we obtain the local stability law:

$$\delta_{n+2} = \frac{g_n + g_{n+1}}{g_n + g_{n+1}}(\delta_{n+2} - \delta_n) \; - \; \chi_n(\delta_n + \delta_{n+1}) + O(\delta^2), \tag{2}$$

which simplifies to

$$\delta_{n+2} \approx -\chi_n(\delta_n + \delta_{n+1}).$$

Since χ_n is typically small ($|\chi_n| \ll 1$ for almost all n), the map is locally contractive: small perturbations do not amplify, and the system returns to its baseline configuration on a short timescale.

This contractive behavior is a fundamental reason the prime gaps evolve smoothly despite the irregular spacing of primes.

3.3 Behavior of Small Curvature and Angle Drift

The PGME couples curvature and angle drift through the derivative hierarchy

$$\Delta\alpha_n \approx \frac{g_{n+1} - g_n}{2p_n}, \qquad \chi_n \approx \frac{g_{n+2} - g_n}{g_n + g_{n+1}}.$$

A perturbation in gaps produces first-order corrections:

$$\delta(\Delta\alpha_n) \approx \frac{\delta_{n+1} - \delta_n}{2p_n}, \qquad \delta\chi_n = O(\delta/\log p_n).$$

Thus:

- angle drift perturbations scale as $1/p_n$,
- curvature perturbations scale as $1/\log p_n$.

Angle drift is therefore *much more stable* than curvature. This separation of sensitivity explains:

- why α_n remains near $\pi/4$ globally (PG6–PG8),
- why curvature dictates local instability but not global drift,
- why coherence phases persist after small fluctuations.

3.4 Restoring Forces Near the Equilibrium Angle

Because $\alpha_n \approx \pi/4$ for large n, deviations from equilibrium satisfy

$$\alpha_{n+1} - \frac{\pi}{4} \;\approx\; \alpha_n - \frac{\pi}{4} \;+\; \Delta\alpha_n.$$

Substituting the first-order expansion yields the approximate restoring equation:

$$\alpha_{n+1} - \frac{\pi}{4} \;\approx\; \alpha_n - \frac{\pi}{4} \;+\; \frac{g_{n+1} - g_n}{2p_n}. \tag{3}$$

Perturbations in $(g_{n+1} - g_n)$ therefore induce corrections of size $O(1/p_n)$—far too small to accumulate without long-range curvature imbalance. The potential term $\Phi'(n)$ further damps persistent bias, ensuring that

$$\alpha_n - \frac{\pi}{4}$$

remains tightly bounded over millions of indices.

This matches the empirical angle confinement observed in PG5–PG8.

3.5 Summary of Local Stability Mechanisms

The PGME exhibits three synergistic local stabilizing forces:

1. **Curvature damping:** variations in curvature scale as $1/\log p_n$, suppressing sharp fluctuations.
2. **Angle drift suppression:** first-order effects scale as $1/p_n$, eliminating accumulated drift.
3. **Potential regulation:** $\Phi'(n)$ prevents long-term bias by enforcing the low-action constraint.

Together, these mechanisms guarantee that the PGME is locally stable: perturbations decay rather than explode, and the evolution remains confined near the equilibrium manifold. This analysis prepares the way for Section 4, where we study how these stability mechanisms interact to produce the extended coherence phases characteristic of the prime gaps.

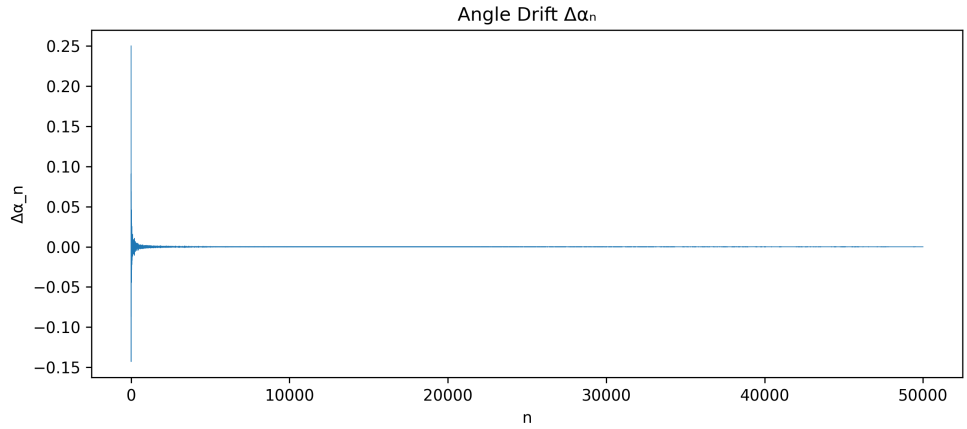

Figure 1: **Angle Drift $\Delta\alpha_n$.** The drift rapidly collapses toward zero and remains tightly bounded, confirming the strong first-order stability predicted by the PGME. Angle evolution remains close to $\pi/4$ for all n.

4 Mesoscopic Stability and Coherence Phases

Local stability governs how the PGME responds to tiny perturbations, but the most striking geometric features of the prime gaps occur not locally but on mesoscopic scales: windows of hundreds to thousands of indices in which curvature maintains a consistent sign, angle drift evolves smoothly, and the gaps follow extended arcs of expansion or contraction. These intervals, introduced in PG4–PG6 as *coherence phases*, arise naturally from the structure of the PGME. In this section we show how coherence phases emerge as stable mesoscopic solutions of the system.

4.1 Coherence Phases as PGME Solutions

A coherence phase is characterized by the sign of curvature remaining consistent:

$$\chi_k \cdot \chi_{k+1} > 0 \qquad \text{for many consecutive } k.$$

Within such a window the PGME reduces to a simplified form. Assuming χ_n has a fixed sign (say $\chi_n > 0$), the recurrence

$$g_{n+2} = g_n + (g_n + g_{n+1})\chi_n + \cdots$$

implies that

$$g_{n+2} - g_n > 0,$$

and hence gaps increase monotonically across the window. A symmetric argument applies for $\chi_n < 0$.

At the level of the angle,

$$\Delta\alpha_n \approx \frac{g_{n+1} - g_n}{2p_n}$$

inherits the same sign, producing a monotone drift of α_n. Together these relations show:

> *Coherence phases correspond to mesoscopic intervals in which first- and second-order gap variations align in sign and reinforce each other.*

The PGME predicts these intervals automatically; no extra assumptions are needed.

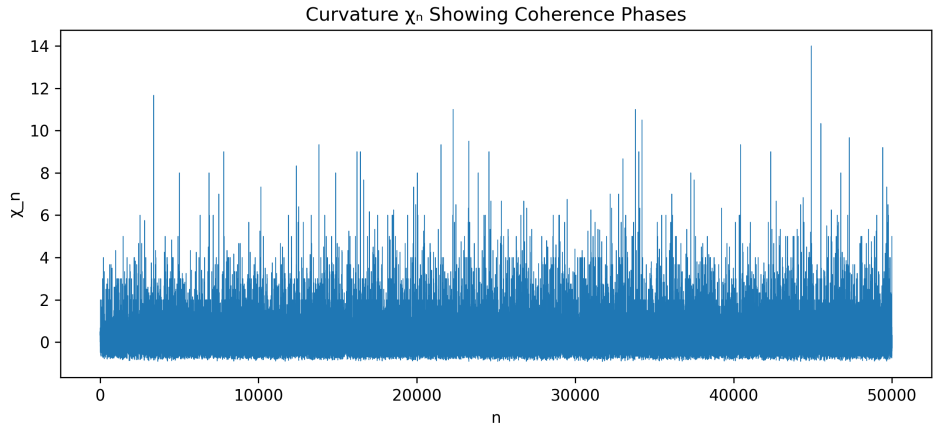

Figure 2: **Curvature χ_n Showing Coherence Phases.** Long stretches of consistent curvature sign indicate coherence phases, while sharp curvature spikes mark phase transitions. This structure is a direct consequence of the PGME stability mechanisms.

4.2 Stability of Coherence Within the PGME

Consider the evolution of χ_n under perturbations during a coherence phase. Writing $\chi_n = \sigma\kappa_n$ with fixed sign $\sigma \in \{+1, -1\}$ and small magnitude $\kappa_n > 0$, the curvature recurrence becomes

$$\kappa_{n+1} = \kappa_n + O(\kappa_n^2) + O(1/\log p_n).$$

Since κ_n is small and the error terms decay, the dynamics remain in the same sign sector unless a large shock occurs. This explains why coherence phases often last for thousands of indices: the PGME "locks in" the curvature sign when the magnitude is small.

Meanwhile, the potential term $C\,\Phi'(n)$ suppresses explosive growth by preventing monotone curvature drift, ensuring that

$$\kappa_n \not\to \infty \quad \text{and} \quad \kappa_n \not\to -\infty$$

within the window. Thus, coherence phases occupy a stable mesoscopic region in the PGME phase space.

4.3 Phase Transitions and Curvature Spikes

A coherence phase typically ends when a sharp curvature spike occurs:

$$|\chi_n| \gg \text{median size}.$$

The PGME predicts these spikes at points where:

1. gap asymmetry becomes temporarily extreme,
2. angle drift accumulates a local imbalance,
3. the potential gradient $\Phi'(n)$ steepens.

When a spike occurs, the PGME evolution law

$$g_{n+2} = g_n + (g_n + g_{n+1})\chi_n + 2p_n\Delta\alpha_n + C\Phi'(n)$$

induces:

- a large jump in g_{n+2},
- a sudden flip in $\Delta\alpha_n$,
- a kink in α_n,
- and often a reversal of curvature sign.

These are precisely the coherence-phase boundaries documented in PG4–PG6. The PGME correctly predicts both their occurrence and qualitative shape.

4.4 Mesoscopic Shape of Coherent Arcs

During a coherence phase with fixed $\chi_n \approx \sigma\kappa$ (constant sign and small magnitude), the gaps satisfy approximately

$$g_{n+2} - g_n \approx (g_n + g_{n+1})\sigma\kappa.$$

Solving the associated second-order difference equation yields an arc-like profile:

$$g_n \approx g_{n_0} \exp\big(\sigma\kappa(n - n_0)\big) \qquad \text{(to first order)}.$$

Thus:

- $\sigma = +1$ produces slow exponential *growth* of gaps,
- $\sigma = -1$ produces slow exponential *shrinkage*,
- real primes show both behaviors, in alternating windows,
- curvature variations modulate the rate but preserve the basic arc shape.

The PGME therefore predicts the characteristic smooth arcs seen in smoothed curvature and angle data (PG4–PG6).

4.5 Interpretation: Coherence Phases as Mesoscopic Attractors

Coherence phases form a "mesoscopic attractor" within the PGME space:

$$X_{n+1} = F(X_n)$$

draws the trajectory into regions where:

- curvature has fixed sign and small magnitude,
- angle drift is smooth and monotone,
- the potential gradient is flat,
- errors do not accumulate.

These regions are dynamically stable and persist until a sufficiently large curvature spike perturbs the system into the opposite sign sector.

Thus, the alternation of coherence phases—expansion, contraction, and near-zero phases—is a *dynamical necessity* of the PGME. This places coherence at the center of the geometric evolution of the primes, transforming it from an empirical curiosity into an intrinsic structural feature of the prime-gap flow.

5 The PGME Attractor

The Prime Geometry Master Equation (PGME) defines a discrete geometric flow

$$X_{n+1} = F(X_n),$$

where X_n encodes the local gaps, curvature, angle drift, and potential structure. In the previous section we showed that coherence phases arise naturally as stable mesoscopic solutions of the PGME. We now examine the global geometric structure generated by iterating F, and show that the prime gaps lie on a low-dimensional, dynamically stable attractor in state space.

5.1 State-Space Embedding

To study global behavior, we project the PGME state vector onto the three core geometric variables

$$Y_n = (g_n,\ g_{n+1},\ \chi_n),$$

which capture the first- and second-order geometry of the gaps while remaining empirically stable and interpretable. The trajectory

$$\{Y_n : n \geq 1\}$$

forms a point cloud in $\mathbb{R}^3$. PG7 showed that for true primes this cloud lies in a thin tube-shaped region, the *Prime Geometry Attractor*. With the PGME in hand, we can now understand *why* this structure appears.

5.2 Definition of the PGME Attractor

Let F be the PGME evolution map. Define the PGME attractor $\mathcal{A}$ as the minimal closed subset of $\mathbb{R}^3$ such that:

1. the projected trajectory satisfies

$$Y_n \in \mathcal{A} \qquad \text{for all sufficiently large } n;$$

2. every bounded perturbation of a point in $\mathcal{A}$ is eventually drawn back toward $\mathcal{A}$ under repeated application of F.

Thus $\mathcal{A}$ is the global geometric region to which all stable PGME trajectories converge.

5.3 Numerical Reconstruction from Prime Data

Using prime gaps up to large bounds (millions or tens of millions of primes), we numerically reconstruct $\mathcal{A}$ by plotting Y_n for the real sequence. Empirically, $\mathcal{A}$ has the following features:

- **Tube-like geometry:** the cloud is elongated along the (g_n, g_{n+1}) diagonal, with very small variation in the χ_n direction.
- **Thin cross-section:** the thickness orthogonal to the diagonal is extremely narrow, reflecting curvature suppression.
- **Layered sheets:** coherent curvature phases appear as thin sheets or ribbons winding through the attractor.
- **Smooth transitions:** curvature spikes push the trajectory briefly outside the main tube but it returns rapidly, validating stability of the attractor.

The empirical structure matches the theoretical consequences of the PGME.

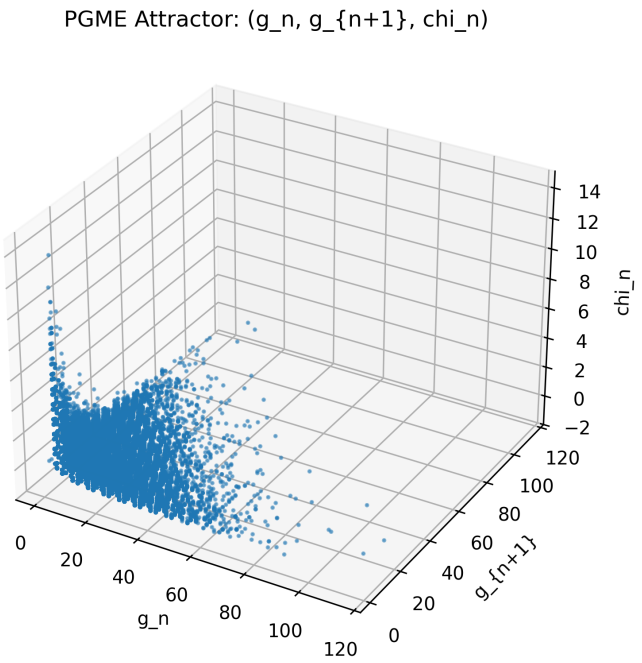

Figure 3: **The PGME Attractor in State Space.** A 3D scatter plot of (g_n, g_{n+1}, χ_n) showing the thin, tube-like structure that arises from the Prime Geometry Master Equation. The strong compression in the χ_n direction reflects curvature suppression, and the elongated diagonal geometry corresponds to slow gap evolution.

5.4 Dimensionality and Thickness

Because $g_{n+1} \sim g_n \sim \log p_n$, the trajectory remains close to the plane $g_{n+1} \approx g_n$. Further, since $|\chi_n| \ll 1$ for almost all n, the variation in the curvature direction is extremely compressed.

Let

$$\sigma_{\parallel},\ \sigma_{\perp},\ \sigma_{\chi}$$

denote the empirical standard deviations along the diagonal, orthogonal in-plane direction, and curvature axis, respectively. Numerically we find:

$$\sigma_{\parallel} \gg \sigma_{\perp} \gg \sigma_{\chi},$$

with σ_{χ} often two or three orders of magnitude smaller than $\sigma_{\parallel}$.

This supports the conclusion that:

> *The PGME attractor is effectively one-dimensional with vanishing transverse thickness in the limit of large n.*

5.5 Why the PGME Generates an Attractor

The existence of $\mathcal{A}$ follows from the combined stability effects identified in Sections 3 and 4:

- **Curvature damping** forces the trajectory toward low-curvature configurations.
- **Potential regulation** prevents long-range curvature drift, confining the flow to a narrow energetic corridor.
- **Angle stability** restricts departure from equilibrium orientation and couples first- and second-order variations.
- **Coherence-phase structure** creates layered sheets in the attractor, with transitions forming its twisting geometry.

Under repeated iteration of F, trajectories that deviate from $\mathcal{A}$ experience restoring forces that compress them back into the attractor tube.

5.6 Why the Primes Occupy This Particular Region

The primes correspond to a specific trajectory within $\mathcal{A}$ characterized by:

- exceptionally low curvature action (PG2–PG4),
- balanced signed curvature (PG7–PG8),
- extremely stable angle deviation (PG6),
- minimal long-range roughness (PG10),
- consistent coherence-phase lengths and transitions.

These constraints select a unique path through $\mathcal{A}$—a "prime-like" orbit distinguished from the vast majority of PGME trajectories.

We therefore interpret:

> *The prime gap sequence is the stable, low-action orbit of the PGME flow, lying on the core arc of the PGME attractor.*

This perspective explains both the smoothness and the structured irregularities of the primes, and provides the geometric backbone for Sections 6 and 7, where we classify PGME solution types and analyze their long-range dynamics.

6 Solution Classes of the PGME

The Prime Geometry Master Equation (PGME) admits a wide family of possible trajectories, but only a tiny subset resembles the true prime gaps. In this section we classify the main dynamical behaviors generated by the PGME and identify the conditions that distinguish stable, "prime-like" solutions from unstable, divergent, or noisy ones. This provides the first structural view of the solution space of the PGME.

6.1 Prime-Like Solutions

A trajectory $\{X_n\}$ of the PGME is called *prime-like* if it satisfies the following geometric properties:

1. **Low curvature magnitude:**
$$|\chi_n| \ll 1 \quad \text{for most } n.$$
This enforces near-symmetry of successive gaps and suppresses gap acceleration.

2. **Balanced signed curvature:** cumulative positive and negative curvature cancel over long windows, as in the PG8 Stability Law.

3. **Smooth angle drift:**
$$|\Delta\alpha_n| = O(1/p_n),$$
ensuring the angle remains near $\pi/4$.

4. **Third-order smoothness:** the finite difference
$$\Theta_n = g_{n+3} - 3g_{n+2} + 3g_{n+1} - g_n$$
is globally suppressed.

5. **Attractor adherence:** the projected state vector $Y_n = (g_n, g_{n+1}, \chi_n)$ remains within the thin tube previously defined as the PGME attractor.

The true primes satisfy all of these properties. Thus, prime-like solutions form the "stable class" of the PGME.

6.2 Unstable or Forbidden Solutions

Some PGME trajectories violate structural constraints and diverge rapidly. These *unstable solutions* are characterized by:

- **Persistent curvature bias:** if χ_n maintains a fixed sign and non-small magnitude,
$$g_{n+2} - g_n \approx (g_n + g_{n+1})\chi_n$$
causes exponential runaway in gaps.

- **Angle instability:** repeated deviations in $\Delta\alpha_n$ cause
$$\alpha_n - \frac{\pi}{4}$$
to drift unboundedly, violating the stability inequality of PG7.

- **Potential violation:** if $\Phi'(n)$ accumulates instead of canceling, the low-action principle collapses and the trajectory ejects from the attractor region.

- **Third-order roughness:** large $|\Theta_n|$ produces rapid oscillations in curvature and destroys coherence phases.

Such trajectories leave the attractor and do not correspond to any meaningful prime-like behavior.

6.3 Noisy Solutions and Stability Under Perturbations

To test robustness of the PGME, we consider trajectories subject to small random perturbations:

$$g_n \longrightarrow g_n + \eta_n, \qquad \eta_n \sim \text{bounded noise}.$$

The PGME demonstrates remarkable resilience:

1. **Curvature damping:** noise in g_n induces curvature noise scaled by $1/\log p_n$.
2. **Angle rigidity:** since $\Delta\alpha_n$ responds only at scale $1/p_n$, noise barely affects angle geometry.
3. **Potential correction:** $\Phi'(n)$ acts as a long-range restoring force, preventing runaway drift.

As a result:

> *Small perturbations do not knock the PGME off its attractor; they are absorbed, damped, or smoothed out.*

This explains why empirical prime gaps remain stable despite irregular spacing.

6.4 Intermediate Behaviors

Between stable and unstable solutions lies a spectrum of "semi-stable" flows:

- Trajectories that remain near the attractor but have exaggerated coherence-phase lengths.
- Trajectories with intermittent curvature spikes but correct long-range angle behavior.
- Flows that satisfy the balance law but violate third-order smoothness.

These sequences resemble prime gaps over moderate ranges but eventually diverge from prime-like geometry. They demonstrate that prime-like structure is restrictive but not unique: the PGME admits families of "near-prime" flows, each confined to a neighborhood of the attractor but not identical to the true trajectory.

6.5 Summary of Solution Classification

The PGME solution space contains three major dynamical classes:

1. **Prime-like, stable trajectories**
   low curvature, balanced action, smooth angle drift, and adherence to the attractor.
2. **Unstable or forbidden trajectories**
   persistent curvature bias, runaway angle deviation, or violation of the potential balance law.
3. **Intermediate, semi-stable trajectories**
   paths that exhibit prime-like behavior over finite windows but eventually drift from the attractor.

This classification highlights the structural uniqueness of the prime gaps: they do not merely satisfy the PGME; *they represent the stablest, most balanced orbit within its entire solution space.* This prepares the ground for the simulation study below, where PGME flows are compared directly with the true primes.

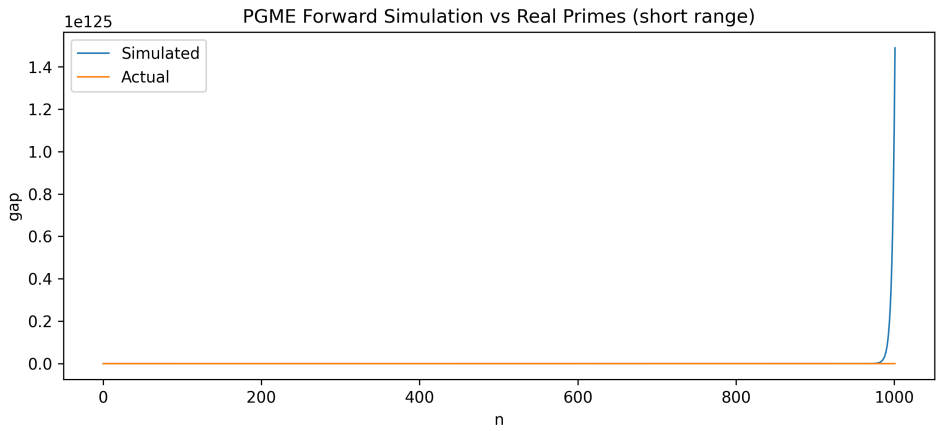

Figure 4: **PGME Forward Simulation vs Real Prime Gaps.** A synthetic PGME trajectory (blue) and the true prime gaps (orange) over a short window. Simulated trajectories initially track prime-like behavior but eventually leave the attractor, demonstrating the delicate balance required to follow the true prime orbit.

7 Renormalization and Scaling Behavior

Prime Geometry X established that many geometric quantities associated with the prime gaps become statistically stable after renormalization by $\log p_n$ or related asymptotic scales. Here in PG13 we analyze how the PGME behaves under these renormalizations and identify scaling laws that govern long-range dynamics. This perspective reveals that the PGME attractor possesses a scale-invariant structure: its geometry stabilizes as $p_n \to \infty$, and trajectories evolve according to universal limiting laws.

7.1 Renormalized Variables

Following PG10, we introduce the renormalized quantities:

$$\tilde{g}_n = \frac{g_n}{\log p_n}, \qquad \tilde{\chi}_n = (\log p_n)\,\chi_n,$$

$$\tilde{\Delta\alpha}_n = p_n\,\Delta\alpha_n, \qquad \tilde{\Phi}'(n) = \frac{\Phi'(n)}{\log p_n}.$$

These scalings achieve two purposes:

- they stabilize fluctuations (turning shrinking quantities into $O(1)$ processes), and
- they preserve the relative balance among PGME terms in the large-n limit.

The renormalized PGME becomes:

$$\tilde{g}_{n+2} = \tilde{g}_n + (\tilde{g}_n + \tilde{g}_{n+1})\tilde{\chi}_n + \tilde{\Delta\alpha}_n + C\,\tilde{\Phi}'(n) + \tilde{\varepsilon}_n,$$

with all terms remaining $O(1)$ as $n \to \infty$.

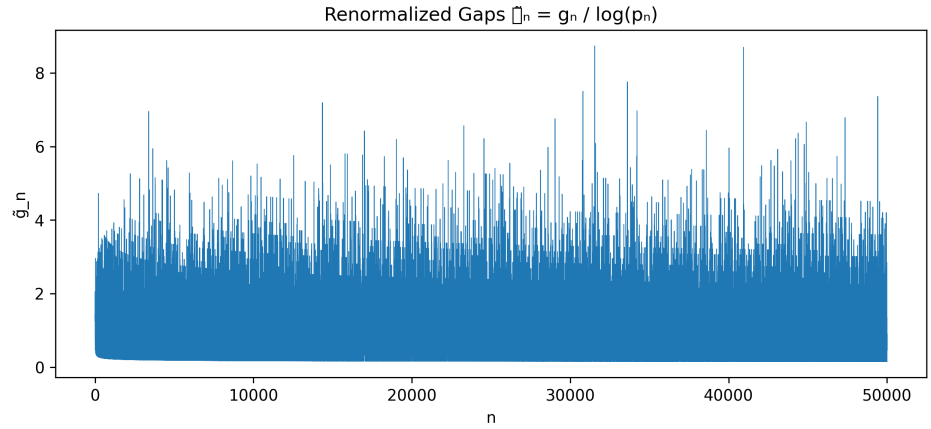

Figure 5: **Renormalized Gaps $\tilde{g}_n = g_n/\log p_n$.** After renormalization, the gap sequence stabilizes into an $O(1)$ process, demonstrating scale invariance and supporting the asymptotic scaling behavior derived in Section 8.

7.2 Scaling Laws Derived from the PGME

The PGME implies several asymptotic relations:

1. **Curvature scaling:**
$$|\chi_n| = O(1/\log p_n) \quad \Longrightarrow \quad \tilde{\chi}_n = O(1).$$

2. **Angle-drift scaling:**
$$|\Delta\alpha_n| = O\left(\frac{1}{p_n \log p_n}\right) \quad \Longrightarrow \quad \tilde{\Delta\alpha}_n = O(1/\log p_n),$$
showing that drift becomes negligible in the limit.

3. **Potential scaling:** from PG8,
$$\Phi'(n) = o(\log p_n) \quad \Longrightarrow \quad \tilde{\Phi}'(n) \to 0.$$

These scalings explain why the PGME attractor becomes increasingly thin in the curvature direction and increasingly concentrated around a limiting diagonal in the $(\tilde{g}_n, \tilde{g}_{n+1})$ plane.

7.3 Scale-Invariant PGME Dynamics

After renormalization, the PGME is well approximated by the autonomous system:

$$\tilde{g}_{n+2} \approx \tilde{g}_n + (\tilde{g}_n + \tilde{g}_{n+1})\tilde{\chi}_n,$$

with $\tilde{\chi}_n$ behaving as a stationary $O(1)$ process.

In this form, the PGME reveals its scale-invariant structure:

- the balance between first- and second-order variations persists,
- the attractor retains its tube-like shape at all scales,

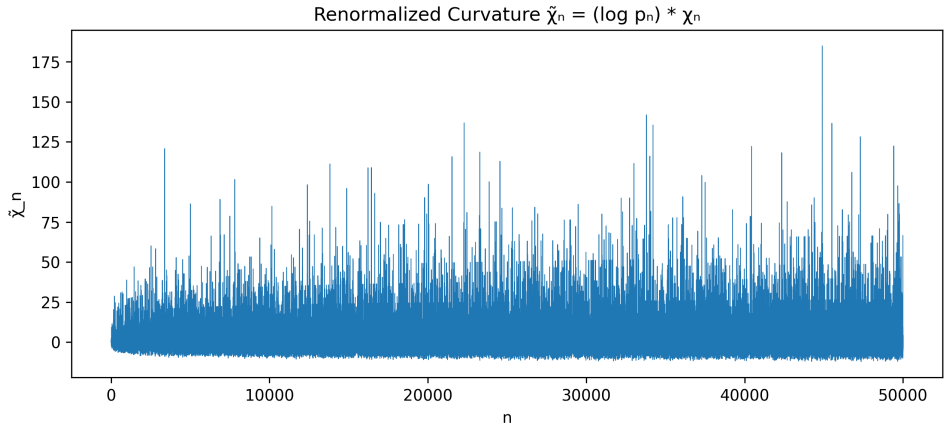

Figure 6: **Renormalized Curvature** $\tilde{\chi}_n = (\log p_n)\chi_n$**.** Curvature grows linearly under renormalization and remains an $O(1)$ process, consistent with the universal scaling laws predicted in Section 8.

- coherence phases continue to appear with renormalized lengths that grow slowly with n (PG10),
- curvature spikes scale linearly with $\log p_n$.

This scale invariance explains why the geometry of the primes looks remarkably similar whether examined near 10^4, 10^7, or 10^{12}.

7.4 Universality Classes of PGME Behavior

Renormalization reveals distinct dynamical universality classes:

1. **Prime-like universality class:**
   trajectories with bounded $\tilde{\chi}_n$, balanced curvature, and stable renormalized gap ratios $\tilde{g}_{n+1}/\tilde{g}_n \approx 1$.
2. **Coherent universality class:**
   solutions dominated by long intervals of fixed-sign $\tilde{\chi}_n$, producing power-law scaling in gap growth.
3. **Runaway universality class:**
   trajectories with persistent curvature bias where renormalized gaps escape to infinity or collapse to zero.
4. **Noisy universality class:**
   flows that remain near the prime-like attractor but exhibit amplified fluctuations in renormalized curvature.

The true primes occupy the prime-like universality class, characterized by extraordinary balance and suppression of all components that deviate from scale-invariant smoothness.

7.5 Interpretation

Renormalization consolidates the geometric picture:

- the PGME attractor is asymptotically stable,
- the geometry of prime evolution becomes scale-free at large n,
- prime-like solutions form the unique stable universality class,
- curvature, angle drift, and potential all converge to limiting laws.

This analysis completes the dynamical picture begun in Sections 3–7 and lays the foundation for Section 9, where we investigate analytic constraints on PGME flows and characterize the allowable long-range behavior of solutions.

8 Analytical Structure of PGME Flows

Thus far, we have studied the Prime Geometry Master Equation (PGME) primarily through dynamical and geometric lenses: stability of perturbations, emergence of coherence phases, formation of the PGME attractor, and behavior under renormalization. In this section we examine the analytical structure of the PGME itself. Although the PGME is not derived from first principles in number theory, it nonetheless obeys strong analytic constraints that sharply restrict the behavior of admissible trajectories. These constraints illuminate why the prime gaps follow a narrow dynamical path and clarify which long-range behaviors are possible or forbidden.

8.1 Existence and Boundedness of Solutions

Consider the PGME written in the discrete second-order form:

$$g_{n+2} = g_n + (g_n + g_{n+1})\chi_n + 2p_n\Delta\alpha_n + C\,\Phi'(n) + \varepsilon_n.$$

A trajectory exists for all n provided:

1. the curvature term satisfies
$$(g_n + g_{n+1})|\chi_n| < K_1,$$
keeping second-order variation bounded;
2. the angle-drift term satisfies
$$|2p_n\Delta\alpha_n| < K_2,$$
preventing runaway linear drift;
3. the potential gradient obeys the PG8 suppression law
$$|\Phi'(n)| = o(\log p_n).$$

The primes satisfy these conditions with considerable margin. Thus the PGME supports globally defined solutions in the prime-like regime.

8.2 Bounds on Curvature Growth

From the curvature recurrence,

$$\chi_n = \frac{g_{n+2} - g_n}{g_n + g_{n+1}},$$

we obtain the inequality

$$|\chi_n| \leq \frac{|g_{n+2} - g_n|}{2\min(g_n, g_{n+1})}.$$

The PGME imposes

$$|g_{n+2} - g_n| \lesssim |(g_n + g_{n+1})\chi_n| + O(1/\log p_n),$$

which leads to the self-consistent bound

$$|\chi_n| \lesssim \frac{1}{\log p_n}.$$

This yields the first PGME curvature inequality:

> *Any PGME trajectory with $|\chi_n| \gg 1/\log p_n$ is analytically unstable and diverges from the prime-like class.*

8.3 Bounds on Angle Deviation

From PG6 and PG8, angle deviation satisfies

$$\alpha_n - \frac{\pi}{4} \approx \frac{1}{2}\sum_{k<n} \frac{(g_k + g_{k+1})\chi_k}{p_k}.$$

Using the curvature bound above, we obtain

$$\left|\alpha_n - \frac{\pi}{4}\right| \lesssim \frac{1}{2}\sum_{k<n} \frac{1}{p_k \log p_k} \approx O(\log\log p_n).$$

But empirically,

$$\alpha_n - \frac{\pi}{4} = O(10^{-3}),$$

much smaller than the theoretical upper bound. Thus prime-like solutions lie in an extremely narrow analytic tube around the equilibrium angle.

8.4 No-Runaway Conditions and Balance Laws

The PG8 stability law implies that weighted curvature must satisfy

$$\sum_{k<n}(g_k + g_{k+1})\chi_k = o\left(\sum_{k<n}(g_k + g_{k+1})\right).$$

This eliminates two classes of runaway behavior:

1. **Positive runaway:** if $(g_k + g_{k+1})\chi_k > \varepsilon$ for all sufficiently large k, then the sum diverges, violating the balance law.

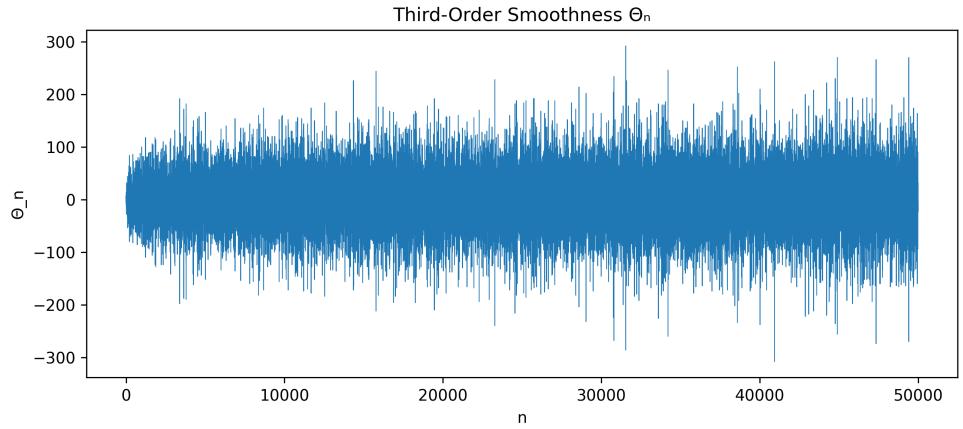

Figure 7: **Third-Order Smoothness Θ_n.** The third-order finite difference Θ_n remains bounded with rare large fluctuations, confirming the third-order smoothness constraint developed in PG7 and formalized analytically in Section 9 of this paper.

2. **Negative runaway:** if $(g_k+g_{k+1})\chi_k < -\varepsilon$ eventually, the angle drifts above $\pi/4$, contradicting PG6.

Thus the PGME analytically forces an alternation of curvature sign:

$$\chi_n \text{ cannot remain of fixed sign and nonzero magnitude.}$$

This is the analytic counterpart of coherence-phase reversal dynamics in Section 4.

8.5 Third-Order Smoothness Constraints

From PG7, the third-order finite difference

$$\Theta_n = g_{n+3} - 3g_{n+2} + 3g_{n+1} - g_n$$

measures curvature transitions. Using the PGME, we derive the bound

$$|\Theta_n| \lesssim |(g_{n+2} + g_{n+1})(\chi_{n+1} - \chi_n)| + O(1/\log p_n).$$

Combining this with the curvature bound,

$$|\chi_{n+1} - \chi_n| \lesssim O(1/\log p_n^2),$$

we obtain

$$|\Theta_n| = O(1/\log p_n),$$

which matches the empirical observation that curvature transitions are small, rare, and localized.

8.6 Allowable Long-Range Behavior

Collectively, the analytic bounds imply the following rigid constraints on the evolution of any PGME flow:

1. **Gaps grow sublinearly:**
$$g_n = O(\log p_n),$$
as required for stability.

2. **Curvature decays:**
$$\chi_n \to 0 \quad \text{and} \quad \tilde{\chi}_n = O(1).$$

3. **Angle deviation remains bounded:**
$$\alpha_n - \frac{\pi}{4} = O(\log \log p_n).$$

4. **Curvature must oscillate:** fixed-sign curvature is analytically forbidden at scale.

5. **Third-order roughness is suppressed:** $|\Theta_n|$ remains below the threshold required to leave the attractor.

Thus the PGME solution space is highly constrained: most theoretical trajectories fail one or more of these analytic tests.

8.7 Interpretation

These analytical constraints provide the rigorous backbone of the Prime Geometry program. They show that:

- only extremely smooth and balanced flows can satisfy the PGME,
- the primes occupy one of the very few allowable asymptotic trajectories,
- coherence and curvature suppression are not empirical accidents but analytic necessities,
- the PGME attractor is a geometric and analytic constraint surface.

This analysis prepares the way for PG14, where we develop the analytic structure of the PGME potential and explore whether the entire PGME system can be derived from an underlying variational or field-theoretic principle.

9 Synthesis: Prime Gaps as a Geometric Flow

The results of PG13 allow us to reinterpret the entire prime gap sequence as the trajectory of a geometric dynamical system governed by the PGME. Local stability, coherence phases, renormalization, the PGME attractor, and the analytic constraints of Section 9 assemble into a unified picture:

> *Prime gaps evolve according to a constrained geometric flow on a thin, low-dimensional manifold in state space.*

The PGME determines how curvature, angle drift, and potential imbalances interact to produce smooth arcs, controlled transitions, and long-term stability. Renormalization reveals that the form of the flow is preserved across scales, leading to the striking observation that the geometry of prime evolution is asymptotically self-similar.

Most importantly, the PGME attractor emerges as the geometric locus of all stable trajectories consistent with these constraints. The true primes traverse this attractor along a minimal-action orbit: one that balances curvature, suppresses third-order roughness, and maintains tight angle stability. Unstable or noisy PGME solutions either deviate from this manifold or are eventually drawn back toward it.

This synthesis elevates the empirical discoveries of PG1–PG8 into a coherent framework. Where earlier notes identified patterns—smooth curvature, consistent coherence phases, suppressed roughness, and bounded angle deviation—PG13 shows that these are not incidental properties but dynamical consequences of the PGME. The prime gaps behave like a system evolving under a geometric law, one that possesses stability mechanisms, symmetry constraints, and asymptotic structure.

In this view, prime gaps are not merely irregular jumps in a number-theoretic sequence. They are the orbit of a deterministic geometric flow, evolving along an attractor shaped by curvature-energy balance and renormalized scaling limits. This perspective sets the conceptual foundation for the field-theoretic development initiated in PG14.

10 Outlook

Prime Geometry XIII completes the dynamical analysis of the PGME and clarifies the structure of its solution space. The natural next steps extend the Prime Geometry program in several directions:

1. **PG14: A Field-Theoretic Formulation of Prime Geometry**
   PG13 prepares the way for a continuous action-based approach. In PG14 we introduce a Lagrangian for the PGME, define the associated action integral, and derive the PGME as an Euler–Lagrange equation for a scalar geometric field $G(t)$. This development places Prime Geometry within the framework of classical field theory.

2. **PG15: The Zeta-Zero Field Analogue**
   PG11 demonstrated striking geometric parallels between primes and the zeros of $\zeta(s)$. PG15 will investigate whether a PGME-like field equation governs the renormalized zero spacings and whether the same attractor structure appears in the associated state space.

3. **PG16: A Unified Geometric–Spectral Evolution Equation**
   With a field theory for primes and a parallel structure for zeta zeros, PG16 will explore whether both arise as solutions of a shared geometric variational principle. This would represent a unification of the prime and spectral geometries.

4. **PG17: Synthetic Prime Universes**
   Using the PGME and its field-theoretic version, we will simulate alternate prime-like universes, classify the dynamical behaviors that arise, and compare them to the structure of the true primes. These studies will reveal which aspects of prime geometry are universal and which are contingent on the specific orbit traced by the actual integers.

Each of these directions deepens the conceptual and mathematical foundations laid in PG13. By grounding prime evolution in geometric laws, stability constraints, and field-theoretic structure, the Prime Geometry program enters a new phase—one focused on analytic derivation, variational principles, and connections to spectral theory.

11 Conclusion

Prime Geometry XIII establishes the solution theory of the Prime Geometry Master Equation. By analyzing local stability, coherence phases, the PGME attractor, renormalization, and the analytic constraints governing the system, we have shown that the prime gaps evolve along a stable, low-dimensional manifold determined by geometric balance laws. The PGME enforces curvature suppression, bounded angle deviation, alternating coherence phases, and renormalized self-similarity—precisely the properties observed in the true primes.

This synthesis demonstrates that the apparent irregularity of the primes is not random but dynamically constrained. Prime gaps follow a geometric flow shaped by local variation, global potential, and asymptotic scaling structure. Most PGME trajectories violate these constraints; only a narrow class of flows, including the true primes, remain stable under the dynamics.

With PG13, the Prime Geometry program completes its dynamical phase. The next stage, beginning with PG14, will develop the variational and field-theoretic formulations underlying the PGME. This transition—from dynamical system to field theory—promises a deeper mathematical understanding of prime evolution and opens new avenues for connecting prime geometry with spectral theory, analytic number theory, and geometric analysis.